extracted several times with Et_2O. The residue was dissolved in acetone and filtered. The acetone dissolution was repeated and the solution refiltered. The porphyrin was then purified by chromatography on 2-mm silica thick layer plates, eluting with 1:1 acetone–THF. The IR, ^1H NMR, and visible spectra were identical with those of **13**.

Acknowledgment. R.C.H. thanks Allied Chemical Co. and the University of Michigan (A. Knoller and M. Gomberg Fellowships) for partial financial assistance. We thank Bernd Soltman for the EI/D mass spectral determinations. Acknowledgment is made to the donors of the Petroleum Research Fund, administered by the American Chemical Society, and the National Science Foundation (Grant CHE 76 23334) for partial support of this research. The National Science Foundation also provided partial support for the purchase of the high-field NMR spectrometer.

Heteroatomic Polyanions of Post-Transition Metals. The Synthesis and Structure of Dithalliumditellurium(2–), $Tl_2Te_2^{2-}$. Skeletal Requirements for Bonding

Robert C. Burns and John D. Corbett*

Contribution from Ames Laboratory—DOE[1] and the Department of Chemistry, Iowa State University, Ames, Iowa 50011. *Received October 6, 1980*

Abstract: Reaction of the alloy composition KTlTe with 2,2,2-crypt in ethylenediamine (en) produces a red-brown solution from which dark brown crystals of $(2,2,2\text{-crypt-}K^+)_2Tl_2Te_2^{2-}\cdot en$ are precipitated by addition of ethylamine. The composition and structure of the crystals were established by single-crystal X-ray diffraction employing 4144 independent reflections ($I > 3\sigma(I)$) collected on an automated diffractometer at room temperature by using monochromatized Mo Kα radiation. The compound crystallizes in space group $P\bar{1}$, a = 12.867 (4) Å, b = 20.957 (3) Å, c = 11.191 (3) Å, α = 90.71 (2)°, β = 112.63 (2)°, γ = 93.24 (2)°, V = 2779 (1) Å^3, and Z = 2. The structure was solved by Patterson and Fourier methods, and positional and thermal parameters of the 62 nonhydrogen atoms were refined to final agreement indices of R = 0.097 and R_w = 0.114. The $Tl_2Te_2^{2-}$ ring has a butterfly shape with the thallium atoms in the fold, a dihedral angle of 49.9°, and Tl–Te distances between 2.929 (3) and 2.984 (2) Å. The last are deduced to be reasonable single-bond separations while the cross-ring distances of 3.600 (3) and 4.414 (3) Å for Tl–Tl and Te–Te, respectively, are plausible nonbonding separations. The anion configuration is considered to derive from a square-planar geometry (D_{2h}) as a consequence of Te–Te nonbonding repulsions, which leads to the diamond shape, and a fold at the thallium atoms because of predominance of p-orbital bonding for that element, yielding internal angles of about 97° and 75° at Tl and Te, respectively. The low stability evident for homopolyatomic species of the heavy post-transition elements in anions of elements to the left of Sn and Pb and in cations for elements before Sb and Bi appears related to skeletal bonding requirements. All known examples, including the polyborane(2–) anions, contain a minimum of somewhat over two p electrons per atom. The use of mixed elements involving one which is more electron-rich accordingly allows the formation of polyatomic anions for the electron poorer elements such as $Tl_2Te_2^{2-}$ for thallium.

In a series of papers reported almost 50 years ago, Zintl and co-workers[2-5] described their extensive electrochemical studies on solutions of sodium metal alloys of many post-transition elements in liquid ammonia. Numerous homopolyatomic anionic species such as Pb_9^{4-}, Sn_9^{4-}, Pb_7^{4-}, Sb_7^{3-}, Bi_5^{3-}, Te_4^{2-}, and Sb_3^{3-} were identified from these investigations in conjunction with the results of exhaustive alloy extractions with the same solvent. However, attempted isolation of the indicated species by evaporation of the ammonia resulted in either amorphous products or normal intermetallic phases, probably because of the greater electron delocalization in, and hence stability of, the metallic phases.

Recently, a general route to the stabilization of some of the above as well as other polyatomic anions has been developed in which the bicyclic 2,2,2-crypt ligand is used to complex the alkali metal cation (Na^+ or K^+) and to prevent electron transfer back from the anion to the cation in the solid state. So far, salts containing the polyatomic anions, Sn_9^{4-},[6] Ge_9^{4-} and Ge_9^{2-},[7] Pb_5^{2-} and Sn_5^{2-},[8] Sb_7^{3-},[9] Bi_4^{2-},[10] and Te_3^{2-}[11] have been isolated from ethylenediamine (en) solution and structurally characterized in these laboratories. In addition, the As_{11}^{3-} anion has recently been so synthesized and structurally characterized by Belin.[12] The anionic species Pb_9^{4-} and Sn_9^{4-} have also been identified by Rudolph and co-workers[13] in liquid NH_3 and en solution by using ^{119}Sn and ^{207}Pb NMR, and mixed-metal M_9^{4-} ions containing both tin and lead were seen as well. Other species containing both tin and antimony were also observed in these NMR studies, although in no case was a solid phase containing the potential heteropolyatomic species isolated. Simultaneously, mixed-metal systems utilizing crypt have been under investigation in these laboratories, seeking to stabilize solids containing heavy elements from the earlier post-transition groups, e.g., mercury and thallium. Zintl and co-workers were not able to obtain any evidence in their studies for homoatomic anions of groups 2 or 3 (i.e., Zn, Cd, Hg, In, and Tl) in ammonia solution,[2] and addition of crypt has in most cases not given significantly better results. The use of mixed heavy

*To whom correspondence should be addressed at Ames Laboratory—DOE.

(1) Operated for the U.S. Department of Energy by Iowa State University under Contract No. W-7405-Eng-82. This research was supported by the Assistant Secretary for Energy Research, Office of Basic Energy Sciences, WPAS-KC-02-03.

(2) Zintl, E.; Goubeau, J.; Dullenkopf, W. *Z. Phys. Chem., Abt. A.* **1931**, *154*, 1–46.
(3) Zintl, E.; Harder, A. *Z. Phys. Chem., Abt. A* **1931**, *154*, 47–91.
(4) Zintl, E.; Dullenkopf, W. *Z. Phys. Chem., Abt. B* **1932**, *16*, 183–194.
(5) Zintl, E.; Kaiser, H. *Z. Anorg. Allg. Chem.* **1933**, *211*, 113–131.
(6) Corbett, J. D.; Edwards, P. *J. Am. Chem. Soc.* **1977**, *99*, 3313–3317.
(7) Belin, C. H. E.; Corbett, J. D.; Cisar, A. *J. Am. Chem. Soc.* **1977**, *99*, 7163–7169.
(8) Edwards, P.; Corbett, J. D. *Inorg. Chem.* **1977**, *16*, 903–907.
(9) Adolphson, D. G.; Corbett, J. D.; Merryman, D. J. *J. Am. Chem. Soc.* **1976**, *98*, 7234–7239.
(10) Cisar, A.; Corbett, J. D. *Inorg. Chem.* **1977**, *16*, 2482–2487.
(11) Cisar, A.; Corbett, J. D. *Inorg. Chem.* **1977**, *16*, 632–635.
(12) Belin, C. H. E. *J. Am. Chem. Soc.* **1980**, *102*, 6036–6040.
(13) Rudolph, R.; Wilson, W. L.; Parker, F.; Taylor, R. C.; Young, D. C. *J. Am. Chem. Soc.* **1978**, *100*, 4269.

0002-7863/81/1503-2627$01.25/0 © 1981 American Chemical Society

metals to form anions allows the exploration of more diverse electronic structures than possible in homoatomic examples, and the present article reports the first example of these, the thallium–tellurium anion system. It should be noted that elements from different periods are utilized so that they may be readily distinguished by X-ray diffraction means.

Experimental Section

Materials and Synthesis. The source of 99.999% thallium and tellurium was United Mineral and Chemical Co. and the "purified" potassium, J. T. Baker Chemical Co. Freshly cut sections of thallium and potassium were prepared and handled only in a drybox. The 2,2,2-crypt (4,7,13,16,21,24-hexaoxa-1,10-diazobicyclo[8.8.8]hexacosane) (Merck) was used as received and was also handled in a drybox. Ethylenediamine (Fisher Scientific Co.) and ethylamine (Eastman-Kodak Co.) were first dried over molecular sieves (Davison, Type 4A) and CaH_2 and then vacuum distilled onto and stored over fresh CaH_2 from which they were distilled immediately prior to use. The ternary alloy composition KTlTe was prepared by fusion of appropriate amounts of the elements at 950 °C in a sealed tantalum tube. Reaction vessels used in these reactions have been described previously.[9]

An alloy of composition KTlTe shows only slight reaction with pure en but reacts immediately in the presence of crypt to give a dark red-brown solution which shows no change with time. A similar reaction occurs in liquid NH_3. Isolation of crystals proved unsuccessful because of an exceptionally high solubility of the product in en, with evaporation yielding a tar-like material, while from NH_3 only a microcrystalline material was obtained. However the reaction product is only marginally soluble in ethylamine, and crystals suitable for X-ray analysis were obtained by addition of ethylamine to an almost saturated solution in en, such that the ethylamine:en ratio was 2:1. When the solution was left standing overnight, large (1–2 mm) block-like dark brown crystals (which appear green in a thin film) formed on the walls of the vessel from the mixed solvent. These were isolated, quickly washed with pure ethylamine, and transferred to a drybox. As the majority of crystals were too large for mounting, they were shattered and selected pieces of a satisfactory size were loaded into 0.3- or 0.5-mm capillaries. Preliminary oscillation photographs suggested that the crystals were single and of low symmetry, but the majority of the investigation was carried out on an automated four-circle diffractometer built in the Ames Laboratory and described elsewhere.[14] The crystal used in this study was block-shaped with dimensions of 0.50 × 0.40 × 0.25 mm.

Data Collection and Reduction. The initial orientation procedure indicated that the crystal was indeed of triclinic symmetry, and data were collected for the predicted cell at ca. 23 °C over the octants HKL, $\bar{H}K\bar{L}$, $\bar{H}\bar{K}L$, and $H\bar{K}\bar{L}$ by using Mo Kα radiation monochromatized with graphite (λ = 0.71002 Å) at a takeoff angle of 4.5°. The intensities of three standards (23.9° < 2θ < 25.6°), each lying approximately along the three axes in reciprocal space, were measured every 75 reflections to check on crystal stability and alignment. The intensities of these reflections decayed anisotropically, with a reduction in integrated intensity of ca. 22% along y^* and ca. 35% along both x^* and z^*. Data were collected out to 2$\theta \leq 50°$ for the first 3475 reflections and to 2$\theta \leq 46°$ for the remainder. A total of 9556 reflections were measured and corrected for decay by using a third-order polynomial as a function of reflection number which was fitted to the sum of the three integrated standards. Corrections were made for Lorentz and polarization effects. After the composition of the material had been established, the data were also corrected for absorption (μ = 70.93 cm^{-1}) by using a ϕ scan method (ϕ = 0–350°, $\Delta\phi$ = 10°) at θ = 11.30° together with a program written by Karcher and Jacobson.[15] The transmission coefficients ranged from 0.56 to 0.99. On accounting for absorption, the final data set consisted of 4144 reflections after averaging with $I > 3\sigma(I)$ and $F > 3\sigma(F)$.

A Howells–Phillips–Rogers test of the intensity distribution of all data gave a strong indication of centricity, after which the space group $P\bar{1}$ was assumed. Precise unit cell parameters were obtained from the same crystal by a least-squares fit to the 2θ values of 15 reflections in the range 24° < 2θ < 32° which were tuned on both Friedel-related peaks to avoid instrument and centering errors. The cell dimensions obtained are a = 12.867 (4) Å, b = 20.957 (3) Å, c = 11.191 (3) Å, α = 90.71 (2)°, β = 112.63 (2)°, γ = 93.24 (2)°, V = 2779 (1) Å^3 for Z = 2, d_{calcd} = 1.86 g/cm^3 and fw = 1554.24.

In passing, it should be noted that in many crypt structures the volume of the unit cell provides a good idea of the number of cations present and, in many cases, the charge on the anion as well, facts which are potentially useful in the structural determination. If the volume occupied by the anion is assumed to be negligible with respect to that of the cryptated alkali metal cation, then the volumes of cryptated sodium and potassium cations are ca. 630 and 660 Å^3, respectively, in a wide range of compounds. In some cases the calculated volume may be somewhat larger, e.g., in the presence of the bulky As_{11}^{3-} anion or if solvent molecules occur in the structure (ca. 30 Å^3 per en per cation).

Structure Solution. Solution of the structure was achieved by conventional heavy-atom Patterson methods, which indicated that the anion was a four-atom species with a butterfly-type geometry. The distribution of intensities of the peaks made it apparent that the anion was heteroatomic and that the heavier thallium atoms were positioned at the fold of the wings. After two cycles of block-diagonal least-squares refinement of positional parameters of the heavy atoms R ($=\sum||F_o| - |F_c||/\sum|F_o|$) was 0.39. An electron density map revealed additional peaks attributable to the potassium, nitrogen, oxygen, and many carbon atoms of the 2,2,2-crypt-K$^+$ cations. After several successive stages of block-diagonal refinement of these positions and isotropic temperature factors alternated with electron density maps, all of the atoms in the cations had been located and R had dropped to 0.24. On introduction of anisotropic temperature factors (of the form $\exp[-(h^2\beta_{11} + k^2\beta_{22} + l^2\beta_{33} + 2hk\beta_{12} + 2hl\beta_{13} + 2kl\beta_{23})]$) for the thallium, tellurium, and potassium atoms R refined to 0.119 after several cycles of full-matrix least squares. At this stage an electron difference map revealed the presence of four peaks located fairly close to the anion which could be attributed to the nonhydrogen atoms of an en molecule. Incorporation of these atoms followed by refinement of all 279 independent parameters using a data set corrected for absorption gave an R of 0.097 and an R_w ($=[\sum w(|F_o| - |F_c|)^2/\sum w|F_o|^2]^{1/2}$) of 0.117, where w was set equal to σ_F^{-2}. Anisotropic temperature factors were then introduced for the nitrogen and oxygen atoms of the crypt ligands, and R_w dropped to 0.116. According to the criteria described by Hamilton[16] this drop in the residual, although outwardly small, is statistically significant at the 99% probability level even though the number of independent parameters has been increased to 359. Examination of $\sum w(|F_o| - |F_c|)^2$ as a function of F_o indicated a slight dependence on the latter, and the data set was reweighted in 50 groups to reduce this effect. This gave final agreement factors, at convergence, of R = 0.097 and R_w = 0.114 (0.090 and 0.104, respectively, for data with 2$\theta \leq 41.5°$). In the final cycle of refinement the largest shift was 0.07σ in the heavy atoms, 0.12σ in the crypt atoms, and 0.07σ in the en atoms. A difference Fourier map was flat to ±0.7 e Å^{-3} except for maxima and minima of 1.7 and −2.6 e Å^{-3} near Tl(2) and 1.2 and −1.8 eÅ^{-3} near Tl(1). These perhaps originate with errors inherent in the absorption correction used as thallium contributes 82% of the value of μ for this compound.

The final residuals for this structure are comparable to, if not generally better than, those for other structures involving polyatomic anions and cryptated alkali metal cations, as also are the standard deviations in the fractional coordinates, bond lengths, and interbond angles. Moreover, as in these other structures, the hydrogen atom positions have not been determined or estimated, leaving 5.2% of the total electron density unaccounted for. Also, it should be noted that no attempt was made to correct for the observed anisotropic decay in the intensities of the reflections. However, in view of the satisfactory outcome of the present determination as well as the size of the data set, little would be gained by collection of a second data set from a cooled crystal.

Sources of all programs, procedures, and the scattering factor data were as previously reported,[9,17] the neutral atom scattering factors also including corrections for the real and imaginary parts of anomalous dispersion. An exception is DISTANCE,[18] a program used to calculate distances and angles, with the standard deviations being estimated from the final cycle of least squares.

Results and Discussion

The final positional and thermal parameters for the 62 nonhydrogen atoms in (2,2,2-crypt-K$^+$)$_2$Tl$_2$Te$_2^{2-}$·en are listed in Table I. All relevant bond distances and angles for the $Tl_2Te_2^{2-}$ anion are given in Table II together with important distances and angles in the 2,2,2-crypt-K$^+$ cations and the ethylenediamine (en) molecule. The remaining distances and angles in the cations and the en molecule as well as a tabulation of the observed and calculated structure factors appear in the supplementary material.

A stereoscopic view of the packing in the unit cell approximately down [$\bar{1}$00] is shown in Figure 1. The stacking of alternate anion and en moieties along z is evident. All interionic (anion–cation)

(14) Schroeder, D. R.; Jacobson, R. A. *Inorg. Chem.* **1973**, *12*, 210–213.
(15) Karcher, B. A.; Jacobson, R. A., personal communication (1980).
(16) Hamilton, W. C. *Acta Crystallogr.* **1965**, *18*, 502–510.
(17) Adolphson, D. G.; Corbett, J. D. *Inorg. Chem.* **1976**, *15*, 1820–1823.
(18) "DISTANCE", provided by W. Jensen, South Dakota State University, 1979, private communication.

Table I. Positional and Thermal Parameters for $(2,2,2\text{-crypt-K}^+)_2Tl_2Te_2^{2-}\cdot en$

atom	x	y	z	β_{11}[a]	β_{22}	β_{33}	β_{12}	β_{13}	β_{23}
Tl(1)	0.2208 (2)	0.3057 (1)	0.9746 (1)	22.7 (2)	3.51 (4)	15.3 (2)	−2.2 (1)	0.0 (1)	1.4 (1)
Tl(2)	0.2093 (2)	0.2336 (1)	0.2601 (2)	33.5 (3)	3.19 (4)	35.2 (4)	−0.2 (1)	25.1 (3)	1.4 (1)
Te(1)	0.2371 (2)	0.1681 (1)	0.0410 (2)	12.3 (2)	3.20 (5)	14.2 (3)	−0.1 (1)	0.9 (2)	0.4 (1)
Te(2)	0.3217 (2)	0.3581 (1)	0.2414 (2)	10.3 (2)	2.85 (5)	16.1 (3)	0.3 (1)	5.3 (2)	−0.3 (1)
K(1)	0.7698 (4)	0.0841 (2)	0.4912 (5)	6.7 (4)	2.0 (1)	9.6 (6)	0.1 (2)	1.6 (4)	0.2 (2)
K(2)	0.7693 (4)	0.3991 (2)	0.3005 (5)	7.9 (5)	2.3 (1)	8.4 (6)	0.3 (2)	3.4 (3)	0.9 (2)
N(11)[c]	0.721 (2)	0.049 (1)	0.213 (2)	10 (2)	2.9 (5)	7 (2)	*b*		
N(12)	0.821 (2)	0.120 (1)	0.771 (2)	9 (2)	3.5 (6)	5 (2)			
N(21)	0.808 (2)	0.396 (1)	0.052 (2)	14 (2)	3.8 (7)	9 (3)			
N(22)	0.735 (2)	0.402 (1)	0.549 (2)	11 (2)	1.7 (4)	12 (3)			
O(11)	0.549 (1)	0.084 (1)	0.307 (1)	10 (2)	2.9 (4)	9 (2)			
O(12)	0.590 (1)	0.099 (1)	0.574 (2)	11 (2)	3.1 (5)	16 (2)			
O(13)	0.800 (1)	0.957 (1)	0.420 (2)	11 (2)	2.6 (4)	14 (2)			
O(14)	0.887 (2)	0.000 (1)	0.687 (1)	17 (2)	1.7 (4)	8 (2)			
O(15)	0.880 (1)	0.155 (1)	0.353 (1)	13 (2)	1.8 (4)	11 (2)			
O(16)	0.895 (1)	0.202 (1)	0.599 (2)	10 (2)	2.5 (4)	13 (2)			
O(21)	0.679 (1)	0.291 (1)	0.124 (2)	12 (2)	2.6 (4)	14 (2)			
O(22)	0.634 (1)	0.307 (1)	0.345 (2)	12 (2)	2.5 (4)	12 (2)			
O(23)	0.996 (1)	0.413 (1)	0.313 (2)	11 (2)	5.0 (6)	14 (2)			
O(24)	0.959 (1)	0.392 (1)	0.537 (2)	7 (1)	3.0 (5)	13 (2)			
O(25)	0.665 (2)	0.486 (1)	0.106 (2)	13 (2)	3.6 (5)	11 (2)			
O(26)	0.670 (1)	0.504 (1)	0.360 (2)	9 (2)	2.7 (4)	13 (2)			

atom	x	y	z	B, Å^2	atom	x	y	z	B, Å^2
C(101)	0.610 (2)	0.072 (1)	0.137 (3)	6.2 (6)	C(203)	0.567 (2)	0.273 (1)	0.120 (3)	5.9 (6)
C(102)	0.521 (2)	0.055 (1)	0.187 (3)	6.0 (6)	C(204)	0.581 (2)	0.253 (1)	0.252 (3)	5.5 (6)
C(103)	0.458 (2)	0.072 (1)	0.350 (3)	6.9 (7)	C(205)	0.631 (2)	0.293 (1)	0.468 (3)	5.9 (6)
C(104)	0.484 (2)	0.117 (1)	0.474 (3)	6.8 (7)	C(206)	0.639 (2)	0.359 (1)	0.536 (3)	5.3 (6)
C(105)	0.614 (2)	0.138 (1)	0.689 (3)	6.8 (7)	C(207)	0.927 (3)	0.418 (1)	0.083 (3)	7.6 (8)
C(106)	0.720 (2)	0.112 (1)	0.799 (3)	6.8 (7)	C(208)	0.012 (3)	0.391 (2)	0.196 (4)	9.4 (9)
C(107)	0.715 (2)	0.978 (1)	0.200 (3)	6.7 (7)	C(209)	0.079 (2)	0.389 (1)	0.425 (3)	7.0 (7)
C(108)	0.818 (2)	0.948 (1)	0.304 (3)	6.3 (6)	C(210)	0.066 (2)	0.413 (1)	0.542 (2)	5.1 (5)
C(109)	0.879 (2)	0.925 (1)	0.525 (3)	5.7 (6)	C(211)	0.947 (2)	0.411 (1)	0.660 (3)	6.0 (6)
C(110)	0.855 (2)	0.934 (1)	0.646 (3)	5.5 (6)	C(212)	0.838 (2)	0.379 (1)	0.654 (3)	5.8 (6)
C(111)	0.884 (2)	0.009 (1)	0.812 (3)	5.9 (6)	C(213)	0.737 (2)	0.440 (1)	0.957 (3)	6.6 (7)
C(112)	0.911 (2)	0.081 (1)	0.851 (2)	5.3 (6)	C(214)	0.728 (2)	0.501 (1)	0.026 (3)	6.1 (6)
C(113)	0.812 (2)	0.077 (1)	0.177 (3)	5.6 (6)	C(215)	0.629 (2)	0.542 (1)	0.149 (3)	5.9 (6)
C(114)	0.842 (2)	0.146 (1)	0.222 (3)	5.8 (6)	C(216)	0.575 (2)	0.522 (1)	0.247 (3)	6.1 (6)
C(115)	0.910 (2)	0.221 (1)	0.396 (3)	6.7 (7)	C(217)	0.624 (2)	0.498 (1)	0.462 (3)	6.1 (6)
C(116)	0.975 (2)	0.223 (1)	0.544 (3)	6.0 (6)	C(218)	0.716 (2)	0.467 (1)	0.577 (3)	6.4 (7)
C(117)	0.953 (2)	0.207 (1)	0.740 (3)	6.5 (7)	N(en) 1	0.379 (4)	0.197 (3)	0.761 (5)	19 (2)
C(118)	0.864 (2)	0.189 (1)	0.797 (3)	5.5 (6)	N(en) 2	0.331 (7)	0.300 (4)	0.632 (8)	29 (3)
C(201)	0.784 (3)	0.330 (1)	0.999 (3)	7.2 (7)	C(en) 1	0.313 (6)	0.241 (3)	0.698 (7)	21 (2)
C(202)	0.667 (3)	0.302 (1)	0.991 (3)	7.2 (7)	C(en) 2	0.431 (6)	0.290 (4)	0.668 (8)	22 (3)

[a] Thermal parameters of the form $\exp[-(\beta_{11}h^2 + \beta_{22}k^2 + \beta_{33}l^2 + 2\beta_{12}hk + 2\beta_{13}hl + 2\beta_{23}kl)]$. $\beta_{ij} \times 10^3$ is listed. [b] Substantially all of the β_{ij} terms for the light atoms were $\leq 3\sigma$. [c] The first digit in parentheses identifies the cation.

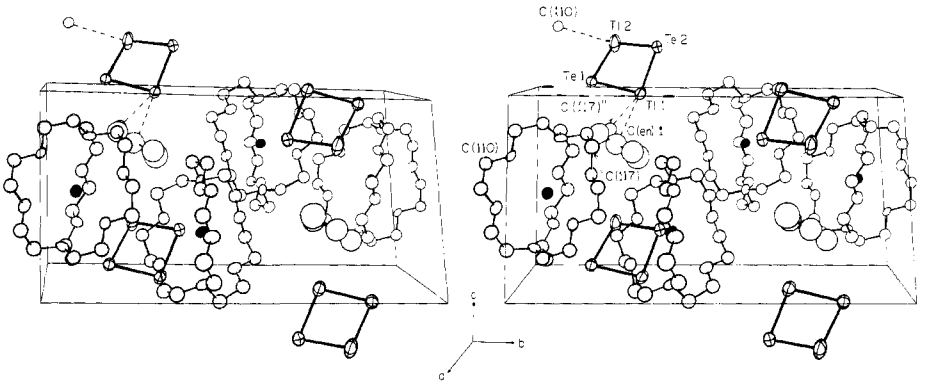

Figure 1. An approximately [$\bar{1}$00] view of the unit cell of $(2,2,2\text{-crypt-K}^+)_2Tl_2Te_2^{2-}\cdot en$. All anions from surrounding formula units with at least one atom in the cell have been included. Thermal ellipsoids are shown at the 30% probability level. The three shortest thallium–carbon distances shown dashed are discussed in the text. (C(110)′ is related to C(110) (x, y, z) by the transformation $1-x, -y, 2-z$ and C(117)″ to C(117) by the transformation $x-1, y, z$.)

and anion–en distances are greater than 3.8 Å (neglecting undetermined hydrogen atom positions) and those distances which appear important to the structure are discussed in detail below.

The conformations of the 2,2,2-crypt-K^+ cations found in this study are comparable to those for symmetry-unconstrained cations found in both $(2,2,2\text{-crypt-K}^+)_2Te_3^{2-}\cdot en$[11] and $(2,2,2\text{-crypt-K}^+)_6Ge_9^{4-}Ge_9^{2-}\cdot 2.5$ en.[7] All of these cations are in turn essentially similar to that found in $(2,2,2\text{-crypt-K}^+)I^-$.[19] Interestingly, there is no real evidence for a shift of either potassium atom toward the end of its associated crypt ligand that is closer to an anion, as previously noted in the Bi_4^{2-} (by 0.09 Å, 3σ) and Te_3^{2-} (by 0.09

(19) Moras, D.; Metz, B.; Weiss, R. *Acta Crystallogr., Sect. B* **1973**, *B29*, 383–388.

Table II. Some Distances and Angles in $(2,2,2\text{-crypt-}K^+)_2Tl_2Te_2^{2-}\cdot en$[a]

Anion

distances			angles			
atom 1	atom 2	Å	atom 1	atom 2	atom 3	deg
Tl(1)	Te(1)	2.984 (2)	Te(1)	Tl(1)	Te(2)	96.54 (7)
Tl(1)	Te(2)	2.929 (3)	Te(1)	Tl(2)	Te(2)	96.75 (9)
Tl(2)	Te(1)	2.945 (3)	Tl(1)	Te(1)	Tl(2)	74.76 (7)
Tl(2)	Te(2)	2.959 (3)	Tl(1)	Te(2)	Tl(2)	75.38 (7)
Tl(1)	Tl(1)	3.600 (3)				
Te(1)	Te(2)	4.414 (3)	dihedral angle, deg			
			Te(1)–Tl(1)–Tl(2)–Te(2)			49.9

Cations and en

distances

atom 1	atom 2	Å	atom 1	atom 2	Å
K(1)	N(11)	3.00 (2)	K(2)	O(21)	2.86 (2)
K(1)	N(12)	3.02 (2)	K(2)	O(22)	2.69 (2)
K(1)	O(11)	2.80 (2)	K(2)	O(23)	2.86 (2)
K(1)	O(12)	2.83 (2)	K(2)	O(24)	2.84 (2)
K(1)	O(13)	2.86 (2)	K(2)	O(25)	2.83 (2)
K(1)	O(14)	2.84 (2)	K(2)	O(26)	2.80 (2)
K(1)	O(15)	2.84 (2)			
K(1)	O(16)	2.85 (2)	N(en) 1	C(en) 1	1.32 (9)
K(2)	N(21)	2.99 (2)	C(en) 1	C(en) 2	1.93 (10)
K(2)	N(22)	3.01 (2)	C(en) 2	N(en) 2	1.23 (11)

angles

atom 1	atom 2	atom 3	deg	atom 1	atom 2	atom 3	deg
N(11)	K(1)	N(12)	179.5 (5)	N(21)	K(2)	N(22)	179.0 (6)
N(11)	K(1)	O(11)	60.3 (5)	N(21)	K(2)	O(21)	60.9 (5)
N(11)	K(1)	O(13)	60.1 (5)	N(21)	K(2)	O(23)	61.1 (6)
N(11)	K(1)	O(15)	59.8 (5)	N(21)	K(2)	O(25)	60.0 (5)
N(12)	K(1)	O(12)	60.4 (5)	N(22)	K(2)	O(22)	60.3 (5)
N(12)	K(1)	O(14)	60.8 (5)	N(22)	K(2)	O(24)	61.6 (5)
N(12)	K(1)	O(16)	60.9 (5)	N(22)	K(2)	O(26)	61.5 (5)
O(11)	K(1)	O(12)	60.3 (5)	O(21)	K(2)	O(22)	59.7 (5)
O(13)	K(1)	O(14)	60.5 (5)	O(23)	K(2)	O(24)	57.9 (5)
O(15)	K(1)	O(16)	59.7 (5)	O(25)	K(2)	O(26)	60.6 (5)
O(11)	K(1)	O(13)	93.7 (5)	O(21)	K(2)	O(23)	101.6 (5)
O(13)	K(1)	O(15)	99.7 (5)	O(23)	K(2)	O(25)	100.1 (5)
O(11)	K(1)	O(15)	98.2 (5)	O(21)	K(2)	O(25)	92.3 (5)
O(12)	K(1)	O(14)	96.0 (5)	O(22)	K(2)	O(24)	97.6 (5)
O(14)	K(1)	O(16)	100.4 (5)	O(24)	K(2)	O(26)	100.2 (5)
O(12)	K(1)	O(16)	97.8 (5)	O(22)	K(2)	O(26)	97.0 (5)

[a] The first digit in parentheses identifies the cation.

Å, 2.3σ) salts. The K–N and K–O distances (Table II) vary from 2.99 to 3.02 (2) Å and 2.80 to 2.86 (2) Å, respectively, except for K(2)–O(22), 2.69 (2) Å, which appears to be significantly shorter than the other distances (by 0.11 Å, 4σ). It should be noted that O(22) also exhibits the shortest anion–(crypt) oxygen interionic distance (3.95 (2) Å) in the structure, in this case to Te(2). Apart from this anomalous distance, the K–N and K–O distances do, however, show a definite tendency toward longer bond lengths than reported for $(2,2,2\text{-crypt-}K^+)I^-$, a trend also found in the Te_3^{2-} salt.

The most interesting aspect of the structure is the anion and its geometry; a butterfly-shaped configuration with the heavier thallium atoms positioned along the fold of the wings. Two views of the anion are given in Figure 2, and the geometry will be discussed in detail below. The thallium–tellurium distances vary from 2.929 (3) to 2.984 (2) Å, with an average of 2.954 Å. The two intermediate Tl–Te distances which involve Tl(2), 2.945 (3), and 2.959 (3) Å, only differ by 3.3σ, while the two extreme distances involving Tl(1) differ by 15σ. The source of the latter effect presumably lies in the close approaches of both C(117), 3.89 (3) Å, and C(en) 1, 3.96 (7) Å (with their undetermined hydrogen atoms) to Tl(1), both from a direction which would exclusively lengthen Tl(1)–Te(1) and shorten Tl(1)–Te(2). The

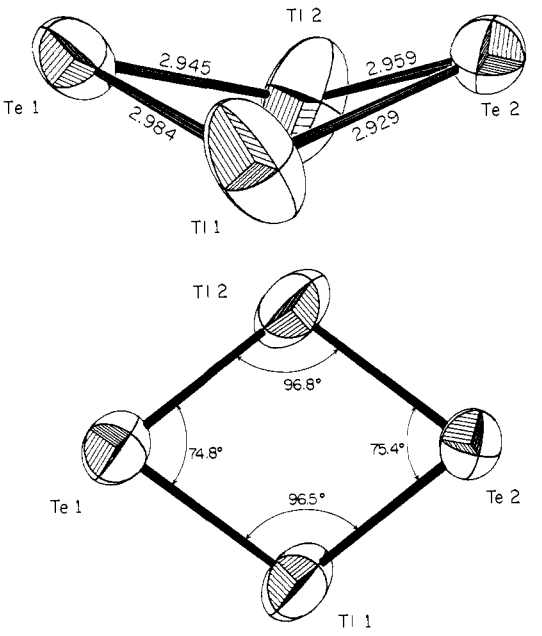

Figure 2. Two views of the $Tl_2Te_2^{2-}$ anion in $(2,2,2\text{-crypt-}K^+)_2Tl_2Te_2^{2-}\cdot en$. Thermal ellipsoids are shown at the 50% probability level.

close approach of the carbon atoms to Tl(1) is also presumably responsible for the reduced thermal parameters of this atom in the pertinent directions relative to those of Tl(2). Although the comparable Tl(2)–C(110) contact (3.81 (3) Å) does not produce a discernible effect on the Tl(2)–Te(2) distance, the approach of this atom does appear to correlate with the reduced thermal motion of Tl(2) in the appropriate direction. These three contacts are shown dashed in Figure 1.

The average Tl–Te distance, 2.954 Å, may be compared with a value of 2.89 Å, calculated from the conventional covalent radius for tellurium (1.37 Å)[20] and a covalent radius of 1.52 Å for thallium, the latter based on the average Tl–C distance of 2.29 Å in $(CH_3)_3Tl$[21] and the covalent radius of carbon (0.77 Å). Use of a covalent tellurium radius obtained from the element[22] (1.42 Å) predicts a Tl–Te distance of 2.94 Å, in slightly better agreement with the observed value. The latter approach may be somewhat less defensible, however, because each directly bonded (divalent) tellurium in the element has four more atoms in neighboring helical chains at 3.495 (3) Å, suggesting some form of weak interaction. This presumably lowers the bond order within each chain by ca. 15% (using Pauling's equation[20]) and causes a small increase in the directly bonded Te–Te distance of about 0.04 Å.

From the calculated covalent radius for thallium (1.52 Å) it is evident that the cross-ring Tl–Tl separation of 3.600 (3) Å in $Tl_2Te_2^{2-}$ does not suggest any substantial bonding interaction. The single-bond metallic distance is similarly smaller, 2.87 Å.[20] One estimate of the van der Waals size of thallium might be based on the size of a $6s^2$ core, with the p orbitals primarily being used for bonding to the tellurium atoms. The transannular van der Waals distance then would be approximated as twice that of Tl^+, 2.68 Å,[20] well less than observed, although this probably represents a low estimate for thallium in an anion. A very approximate van der Waals distance for the neutral atom ($6s^26p^1$) of 1.9–2.0 Å may be obtained from trends in such distances for the p-block elements as given by Bondi.[23] However, this estimate includes a contribution from the 6p valence orbitals and is less appropriate here as these orbitals are believed to be used primarily in skeletal bonding. Thus the former estimate is more consistent with the bonding interpretation to be proposed for this anion. ESR

(20) Pauling, L. "Nature of the Chemical Bond", 3rd ed.; Cornell University Press: Ithaca, NY, **1960**.
(21) Sheldrick, G. M.; Sheldrick, W. S. *J. Chem. Soc. A* **1970**, 28–30.
(22) Cherin, P.; Unger, P. *Acta Crystallogr.* **1967**, *23*, 670–671.
(23) Bondi, A. *J. Phys. Chem.* **1964**, *68*, 441–451.

measurements on the compound at both room temperature and −196 °C gave no evidence for any unpaired spin density.

Formally, the anion may be represented by the localized valence bond representation given below, although this does not provide a rationale for the folded diamond shape of the anion.

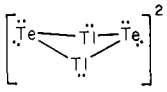

The observed geometry for the 20 valence-electron $Tl_2Te_2^{2-}$ anion illustrates an alternative to the well-known tetrahedron with four topologically equivalent atoms and 20 valence electrons, e.g., P_4. However, rather than consider the geometry of the anion in terms of an opened tetrahedron, the comparison is clearer when pursued from a square-planar geometry to which the anion is more readily related.

In an A_4 system of D_{4h} symmetry the π-manifold (which is orthogonal to the σ system and encompasses the np valence orbitals on each atom) contains a_{2u}, e_g, and b_{2u} orbitals in order of decreasing energy (stabilization). In species such as Te_4^{2+} and Bi_4^{2-}, each with 22 valence electrons, the a_{2u} and e_g orbitals are filled and there is a large energy gap between the filled e_g and unfilled b_{2u} levels.[24] With two fewer valence electrons the e_g level would be only half-filled but, under D_{2h} symmetry, as in a planar version of the $Tl_2Te_2^{2-}$ anion with 90° bond angles, the e_g level is split ($e_g \rightarrow b_{2g} + b_{3g}$) and the π manifold is now b_{1u}, b_{2g}, b_{3g}, and b_{1u}.

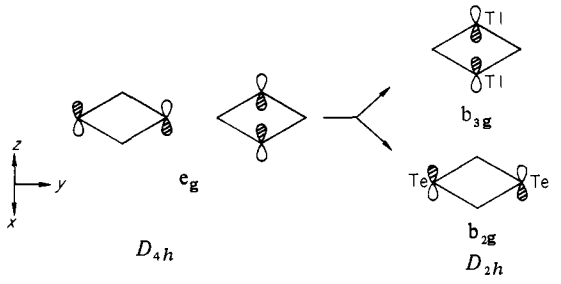

For such an anion the b_{2g} level, which is associated only with the tellurium atoms, is expected to lie below the b_{3g} level, associated only with thallium, because of the relatively higher binding energy of the valence orbitals of tellurium. The formal population e_g^2 in D_{4h} thus becomes b_{2g}^2 in D_{2h}, giving a singlet ground state provided that the energy gap between b_{2g} and b_{3g} is greater than, say, 2–3 eV. Some idea of the relationship between the energies of these two MO's is given by the valence-state ionization energies of the np electrons for the gaseous elements, ca. −6.8 and −9.8 eV for thallium and tellurium, respectively.[25]

At this stage in the argument the problem becomes a question of energetics rather than one of symmetry. Potentially, there are three ways of increasing the energy gap between the b_{2g} and b_{3g} levels, and the acceptable modes will be those which do not lead to a decrease in total stabilization energy for the anion. These processes are the formation of two cross-ring (transannular) bonds as a result of extensive out-of-plane atomic displacements and either in-plane bond length or bond angle distortions.

The first of these possibilities effectively gives rise to a distorted (D_{2d}) tetrahedron but would lead to a partitioning of charge (in the valence bond sense) to give formal positive and (large) negative charges on the tellurium and thallium atoms, respectively. Even allowing for the considerable charge flow that would necessarily occur, this must be an energetically unfavorable process. The alternate formation of only one transannular bond would in either case give an unacceptable diradical species. The second process, in-plane bond length distortions to give alternations in bond length around the ring, would be expected to have little or no effect on the total stabilization energy of the anion. The third choice, bond angle distortions, may involve either in-plane or out-of-plane displacement of the atoms. While D_{2h} symmetry is maintained, the energy gap between the b_{2g} and b_{3g} levels may be easily enlarged by increasing the Te–Te distance while decreasing the Tl–Tl separation. Note that in square-planar $Tl_2Te_2^{2-}$ the Te–Te distance would by 4.18 Å and that twice the van der Waals radius for tellurium as given by Bondi[23] is 4.20 Å. This repulsion would produce the observed diamond shape of the anion. However, it is difficult to estimate, a priori, the magnitude of the increase in separation between the b_{2g} and b_{3g} valence levels for a particular amount of distortion and whether or not the total stabilization energy increases or decreases.

Now for the species which contain tellurium, the bond angle at this element has been found to vary from 113.1° in Te_3^{2-} to ca. 60° in the cationic species $Te_3S_3^{2+}$ and Te_6^{4+}, although in the latter examples the bonds are likely to be bent.[11,26,27] The wide range of angles found therefore suggests that the 75° bond angles observed at tellurium in $Tl_2Te_2^{2-}$ have little effect on the extent of distortion. Rather the bond angles at thallium constitute at least *one* determining factor in this process. As the distortion progresses, the angles at thallium increase, suggesting an increase in s orbital involvement (or hybridization) in the bonding. This should be relatively unfavorable in view of the large s → p promotion energy for thallium and relatively less favorable overlap for heavier elements, reasons why this element is usually judged to employ primarily p orbitals in covalent bonding.[28] One way of avoiding this is for the anion to fold along the Tl–Tl vector as the Te–Te distance increases so that thallium maintains a bond angle nearer 90° (96.6° observed). (Visualizing the fold to occur along the Te–Te vector is of course equivalent.) The symmetry of the anion is then C_{2v}.

Importantly, it should be noted that incorporation of the fold also introduces some "s" character into the b_{2g} and b_{3g} orbitals on tellurium and thallium, respectively, and, as the s → p separation is larger for tellurium than for thallium (ca. 7.8 vs. 6.7 eV, respectively[25]), this also increases the energy gap between the original b_{2g} (now b_1) and b_{3g} (now b_2) levels. However, if this bending process is continued far enough, there will be a destabilizing (antibonding) interaction between "p-type" lobes of the orbitals originally derived from b_{2g} on tellurium and b_{3g} on thallium, the antithesis of the desired effect. The observed fold is actually a modest 50°.

While the above arguments are not rigorous, they do permit a reasonable rationale of some of the major aspects of the observed geometry. In particular, the energy difference between the b_{2g} and b_{3g} orbitals is reasoned to increase on distortion of the original square-planar geometry by both an in-plane change in the bond angles *and* by folding along the Tl–Tl (or Te–Te) vector. This increase is more likely to produce a singlet ground state. However other factors such as the effect of possible stereochemical activity of the lone pairs on the thallium atoms have not been directly considered, and a more extensive analysis of the $Tl_2Te_2^{2-}$ anion would be required to shed light on these and other aspects of the structure.

The electronic requirements of polyatomic species of the early post-transition elements appear to impose considerable restrictions on their stability. Indeed, Zintl and co-workers[2] were not able to obtain significant evidence in liquid NH_3 for polyanions of elements to the left of group 4, specifically for Cu, Ag, Au, Zn, Cd, Hg, and Tl. Instead, only insoluble sodium alloys or the free elements plus sodium dissolved in NH_3 were obtained in their titrations, although the method did provide a convenient synthetic route to some new alloys. In fact, only with germanium has the addition of crypt had the effect of stabilizing species in en for which the Zintl group found only limited evidence for any anions when working in liquid NH_3.[7] However, the general stabilizing effect that crypt complexation has on many Zintl-type polyanion systems

(24) Tanaka, K.; Yamabe, T.; Terama-e, H.; Fukui, K. *Inorg. Chem.* **1979**, *18*, 3591–3595.
(25) Calculated from data in Moore, C. E. *Natl. Stand. Ref. Data Ser. (U.S., Natl. Bur. Stand.)* **1971**, *NSRDS-NBS 35*.
(26) Gillespie, R. J.; Luk, W.-C.; Maharajh, E.; Slim, D. R. *Inorg. Chem.* **1977**, *16*, 892–896.
(27) Burns, R. C.; Gillespie, R. J.; Luk, W.-C.; Slim, D. R. *Inorg. Chem.* **1979**, *18*, 3086–3094.
(28) Drago, R. J. *J. Phys. Chem.* **1958**, *62*, 353–357.

is not found with those elements which occur to the left of lead, specifically Au, Hg, and Tl.[29] Surprisingly, K–Au alloys (which generally reduce en and ethylamine) yield a *white* solid which contains the alloy components and crypt when NH_3 solutions of the same materials are evaporated at low temperatures. This product is unstable above ca. −10 °C, giving metallic gold and other (unidentified) products.[29] It is tentatively suggested that this solid contains the monoatomic Au^- anion with the electron configuration $5d^{10}6s^2$. Recently, Lagowski and co-workers have reported that a gold anion, also suggested to be Au^-, forms in NH_3 solutions without crypt, where it has been studied by spectroscopic and electrochemical procedures.[30,31]

Our studies of mercury and thallium alloys with NH_3, en, and ethylamine as solvents have given no evidence for homopolyatomic species; for example, attempted anion preparations from alloys such as KHg, KHg_2, KTl, and K_4Tl_5 merely result in the extraction of potassium and the formation of more mercury- or thallium-rich alloys, with the composition of the resulting alloy being dependent on the state of subdivision of the original material, the temperature at which the reaction was run, and whether crypt was present.

It is believed that this general behavior stems from the paucity of p electrons in these elements together with the fact that bonding in polyatomic species of this type appears to involve primarily the 6p orbitals. Assuming that each metal atom in a potential polyatomic cluster has an exo-skeletal lone pair which is primarily s^2 and that the smallest polytopal moieties are typified by the *closo*-borane species $B_nH_n^{2-}$ with their usual requirement of $2n + 2$ skeletal electrons, one finds a range of 2.50–2.17 p electrons per element are required between the (unknown) $B_4H_4^{2-}$ and $B_{12}H_{12}^{2-}$ anions, respectively. This electronic complement indeed appears to be similar to that in structurally known homopolyatomic anions of tin and lead, namely, Sn_4^{2-} [32,33] (2.50), Sn_9^{4-} (2.44), and Sn_5^{2-} and Pb_5^{2-} (2.40), notwithstanding that the bonding in these heavy element clusters must certainly be weaker than in the boranes. Accordingly, in order for discrete polyatomic systems to form from electron-poor elements such as mercury and thallium, extremely high and energetically unfavorable anionic charges would be required to make up the necessary complement of skeletal electrons such as Hg_4^{10-} and Tl_4^{6-} for the tetrahedral species with 2.5 p electrons per atom.

It is worth noting that a minimum electron concentration of about 2.4 p electrons per atom suggested by the known homopolyatomic anions of tin and lead also applies to the stability of the (frequently isoelectronic) homopolyatomic *cations* of the group 5 and 6 elements.[34] Particularly bismuth, sulfur, selenium, and tellurium are rich in the number of homopolyatomic cations they form under acidic conditions, again with a minimum of about 2.4 p electrons per atom (in Bi_5^{3+}). Extensive studies of analogous systems involving earlier elements, tin and lead especially, reveal that any polyatomic cations of these elements are strikingly less stable. This is consistent since any such cation would have fewer than two p electrons per atom.

In passing it should be noted that isolated tetrahedral Tl_4 and Sn_4 units are known in alloy systems, viz., in Na_2Tl and KSn.[35,36] These tetrahedra would be formally isoelectronic with P_4 (3.0 p electrons per atom) only when considered in the (unrealistic) limit of complete electron transfer from the alkali metal to the cluster (Tl_4^{8-}, Sn_4^{4-}). (The possibility of 18-electron Tl_4^{6-} and Sn_4^{2-} species in these phases should also be considered.) The anionic unit in the real systems doubtlessly has a lower electron density through delocalization of some of the high charge back onto the cations, particularly with thallium. Similarly, isolated square-planar Hg_4 units in Na_3Hg_2 [37] would with complete electron transfer attain a hypothetical closed-shell configuration at Hg_4^{6-} with only 1.5 p electrons per atom.[38] Again, charge transfer to the cation is evident from both symmetry and physical properties, in this case from π-type orbitals. Indeed, there are many such clusters which are known in solid alloys but evidently not in solution, presumably favored by a relatively high concentration of electrons which preserves a sufficient amount of σ bonding in the solid state and hence the basic cluster shape.

Clearly one way to stabilize discrete polyanions of elements like mercury and thallium with their relatively low valence electron counts is to combine them with more electron-rich elements. It was this concept which led to the present study and toward continuing efforts. Of course, oxidation–reduction reactions in solution are likely to be quite complex in heteroatomic systems of this type and the phase composition of the ternary alloys is generally unknown as well, so that the course of any reaction is fairly unpredictable at our present level of understanding of mixed element anions. For example, thallium appears to form heteropolyatomic anions with tin as well as tellurium but not with antimony,[29] while Rudolph and co-workers have also observed mixed anion species in more electron-rich systems by using NMR such as those involving Sn–Pb and Sn–Sb[13] and also Sn–Bi and Sn–Tl.[33]

Acknowledgment. We thank Professor R. A. Jacobson and the members of his research group for the use of the diffractometer and for many helpful suggestions during the refinement of the structure. We also acknowledge the assistance of Professor R. Rudolph in informing us of the results of recent studies prior to their publication.

Supplementary Material Available: A listing of structure factor amplitudes and additional bond distances and interbond angles in the cations (14 pages). Ordering information is given on any current masthead page.

(29) Burns, R. C.; Corbett, J. D.; Armatis, F., Jr., unpublished observations.
(30) Peer, W. J.; Lagowski, J. J. *J. Am. Chem. Soc.* **1978**, *100*, 6260–6261.
(31) Teherani, T.; Peer, W. J.; Lagowski, J. J.; Bard, A. J. *J. Am. Chem. Soc.* **1978**, *100*, 7768–7770.
(32) Critchlow, S. C.; Corbett, J. D. *J. Chem. Soc., Chem. Commun.* **1981**, 236–237.
(33) Rudolph, R. W., personal communication (1980).
(34) Corbett, J. D. *Prog. Inorg. Chem.* **1976**, *21*, 129–158.
(35) Hansen, D. A.; Smith, J. F. *Acta Crystallogr.* **1967**, *22*, 836–845.
(36) Hewaidy, I. F.; Busmann, E.; Klemm, W. *Z. Anorg. Allg. Chem.* **1964**, *328*, 283–293.
(37) Nielson, J. W.; Baenziger, N. C. *Acta Crystallogr.* **1954**, *7*, 277–282.
(38) Corbett, J. D. *Inorg. Nucl. Chem. Letters* **1969**, *5*, 81–84.